Supplementary information:

Quantification of gold nanoparticle accumulation in tissue by two-photon luminescence microscopy

*Jordi Morales-Dalmau[1], Clara Vilches[1], Vanesa Sanz[1], Ignacio de Miguel[1], Valeria Rodríguez-Fajardo[1], Pascal Berto[1], Mar Martínez-Lozano[2], Oriol Casanovas[2], Turgut Durduran[1,3] and Romain Quidant[1,3]**

1. ICFO – Institut de Ciències Fotòniques, The Barcelona Institute of Science and Technology, 08860 Castelldefels, Barcelona, Spain.
2. ProCURE - Catalan Institute of Oncology, OncoBell – IDIBELL, Tumor Angiogenesis Group, 08907 Hospitalet de Llobregat, Barcelona, Spain.
3. ICREA - Institució Catalana de Recerca i Estudis Avançats, 08010 Barcelona, Spain.

KEYWORDS: two-photon luminescence, microscopy, gold nanoparticles, nanotechnology, nanomedicine, in vitro, in vivo

GOLD NANOROD SYNTHESIS IN CETYL TRIMETHYL AMMONIUM BROMIDE

Gold nanorods (GNR) were grown in-house in suspension using a slightly modified seed-mediated method in cetyl trimethyl ammonium bromide (CTAB, Sigma-Aldrich) and maintained at 31ºC. The final size of the GNRs was 11 nm x 44 nm with an absorption peak corresponding to the longitudinal surface plasmon resonance (LSPR) around 830 nm.

In order to study the dependence of two-photon luminescence signal, two types of surface chemistry were analyzed. Polyethylene glycol (PEG) is one of the most used surface coatings to enhance stability and biocompatibility of GNRs *in vitro* and *in vivo* without specific tumor

targeting[1–5]. On the other hand, arginylglycylaspartic acid (RGD) is used as surface functionalization of GNRs to target $\alpha_v\beta_3$ integrins, which are over-expressed in different types of tumors[1,3,6–8].

GOLD NANOROD POLYETHYLENE GLYCOL FUNCTIONALIZATION

The GNRs suspension in CTAB was ultra-centrifuged (Avanti J-E rotor JA-25.50, Beckman Coulter, USA) for 25 min at 23708 xg (14000 rpm) and at 31°C; then, the excess of CTAB was removed by eliminating 90% of the supernatant. The next step was to carry out the ligand exchange reaction by mixing in double purified water (MilliQ, Merck KGaA, Germany) 50% v/v of citrate 0.1 M pH 4 (C3434 Sigma, USA), 3000 Da polyethylene glycol (PEG, PEG1099, Iris Biotech, Germany) at 1 mg/mL and the concentrated GNRs-CTAB at 0.25 OD/mL. The mixture was sonicated for 30 minutes and kept at 28°C overnight to allow the exchange of CTAB chains and PEG moieties. The PEGylated solution (GNRs-PEG) was ultra-centrifuged (25 min at 23708 xg and at 28°C) to remove unbounded PEG moieties, filtered (25 mm RC syringe filter, 0,2 μm pore size, Corning Inc, USA) to discard aggregation, washed twice and diluted with double purified water (MilliQ, Merck KGaA, Germany) to the desired final concentration.

GOLD NANOROD ARGINYLGLYCYLASPARTIC ACID FUNCTIONALIZATION

GNR-PEG suspension was centrifuged at 14000 rpm for 10 minutes, decanted and re-dispersed in a solution with 1-Ethyl-3-(3-dimethylaminopropyl)carbodiimide (EDC, E6383, Sigma-Aldrich) and sulfo-N-hydroxysuccinimide (sulfo-NHS, 56485, Sigma-Aldrich). After 1 hour, the suspension was centrifuged at 14000 rpm for 10 minutes to remove the excess of ECD/sulfo-NHS and the activated GNRs were mixed with the peptide ligand

arginylglycylaspartic acid (RGD, G4391, Sigma-Aldrich) in Mili-Q water and activated at 37^{o}C in an overnight process.

SPECTRUM CHARACTERIZATION OF GOLD NANORODS

Ultraviolet-visible absorption spectra of GNRs in Milli-Q water suspension were acquired with a microplate reader (Synergy H1, BioTek Instruments, Inc.). Optical density (OD) spectra were collected from 400 nm to 1000 nm, using 96 well plates (polystyrene, clear, flat bottom, Nunc MicroWell, Thermo Fisher Scientific) with 0.69 cm path length (250 μL of studied volume). Water spectrum subtraction and triplicates were done for each sample. For toxicity, uptake and TPL study, GNR concentration was determined as $c = OD/(l \cdot \epsilon)$, where c (mol/L) is the molar concentration, OD (a.u.) is the optical density, l (cm) is the path length of the cuvette and ε (1/(cm·mol/L)) is the GNR molar extinction coefficient. Same ε was considered for the three surface chemistries (CTAB, PEG and RGD). The self-normalized optical density (OD) spectra of GNRs in suspension functionalized with CTAB, PEG or RGD were shown in *Figure S1*. The localized surface plasmon resonance peak of GNR-CTAB was 20 nm red-shifted compared to GNR-PEG and GNR-RGD (830 nm, 810nm and 810 nm, respectively). Results showed that GNRs were stable during different functionalization steps.

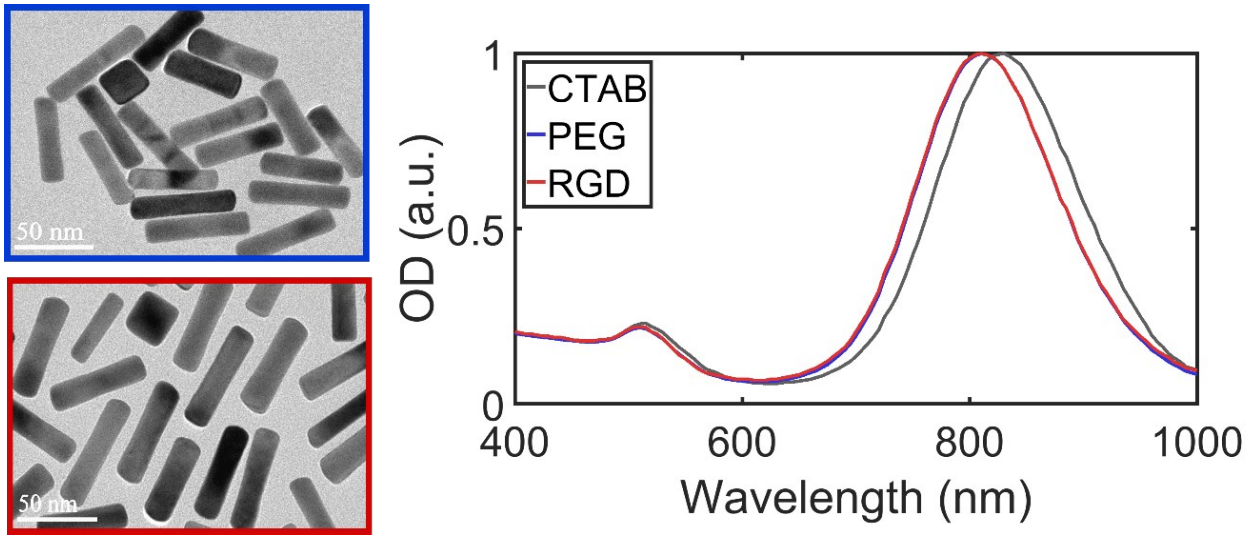

Figure S1. Self-normalized optical density (OD) spectra of GNRs functionalized with CTAB, PEG and RGD, and transmission electron microscopy images of GNR-PEG (in blue) and GNR-RGD (in red). The absorption peak of GNR-CTAB, GNR-PEG and GNR-RGD was centered at 830 nm, 810 nm and 810 nm, respectively.

CELL TYPE AND SAMPLE PREPARATION

A 786-O (human clear cell renal cell adenocarcinoma, ATCC CRL-1932) cell line were cultured in Dulbecco's Modified Eagle Medium (DMEM) and Roswell Park Memorial Institute (RPMI) 1640 media supplemented with 10% fetal bovine serum (FBS) and maintained at 37ºC and 5% CO_2. Passages were done when cultured flasks reached 80% confluency.

For cytotoxicity and uptake experiments, 5000 cells per well were seeded in 96 well plates (flat bottom, Corning Inc.) and let grown for two days. Eventually, each well contained 20000 cells before incubation with GNR-PEG or GNR-RGD. In all *in vitro* experiments, 100 µL of GNR diluted in appropriate culture medium without FBS were added at specific concentration to each well.

CYTOTOXICITY

Cytotoxicity of GNR-PEG and GNR-RGD were assessed at different molar concentrations (from 0.01 nM to 10 nM) after 24 hours of incubation, and after different hours of incubation (1h, 6h and 24 hours) at 1 nM. After the incubation period, 20 μL of 5 mg/mL thiazolyl blue tetrazolium bromide (MTT, M2128, CAS 298-93-1, Sigma-Aldrich) were added to each cell well. Plates were incubated at 37ºC and checked every 30 minutes until visualization of formazan crystal formation (~75-90 minutes). MTT solution was then carefully removed and cells were homogenized in 150 μL of dimethyl sulfoxide (DMSO) to dissolve formazan crystals. Absorbance was measured at 550 nm on a microplate reader (Synergy H1, BioTek Instruments, Inc.). All plates included appropriate control alive/dead cells and eight replicas of each condition. Cellular viability was calculated by extracting the mean MTT signal of the dead control group from the MTT signal from each studied condition and normalized by the mean MTT signal from the alive control group.

Cell viability from GNR-PEG and GNR-RGD incubated with 786-O cells at 1 nM was maintained around 100% during the first 24 hours (Figure S2(a)). In addition, cell viability was higher than 50% (considered cytotoxic) after 24 hours of incubation even at the largest tested concentration of both functionalizations (5 nM, Figure S2(b)). These results were compatible with the observed from other recent studies in our group with GNR-PEG incubated with different cancerous cell lines (data not shown).

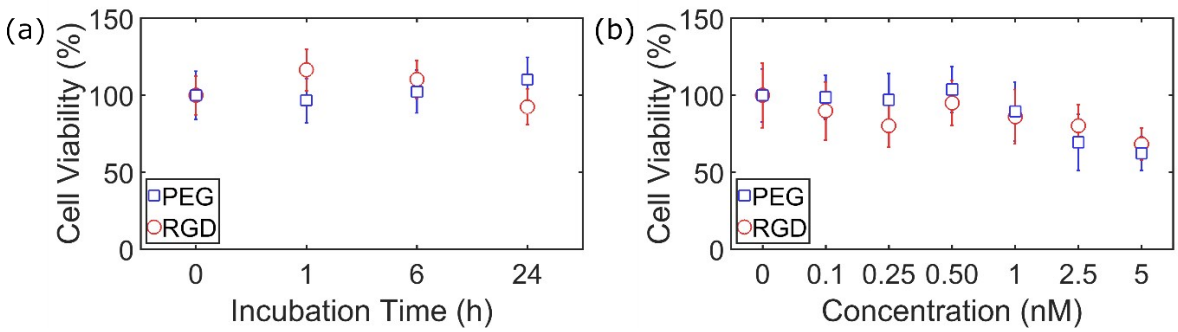

Figure S2. Cell viability (%) measured with MTT from the incubation of GNR-PEG and GNR-RGD with 786-O cells at different experimental conditions. (a) Cell viability at different incubation times (0 h, 1 h, 6 h and 24 hours) at 1 nM. (b) Cell viability at different concentrations (0 nM, 0.1 nM, 0.25 nM, 0.5 nM, 1 nM, 2.5 nM and 5 nM) after 24 hours of incubation. No cytotoxic effects were presented in 786-O cell line (cell viability >50%).

IN VITRO UPTAKE QUANTIFICATION OF GOLD NANORODS

Representative images of the uptake of GNR-PEG and GRN-RGD 24 hours after incubation with 786-O cells were included in Figure S3 and Figure S4. Differences in TPL intensity between the two functionalizations showed the potential of TPL to quantify and distinguish different nanoparticle distribution.

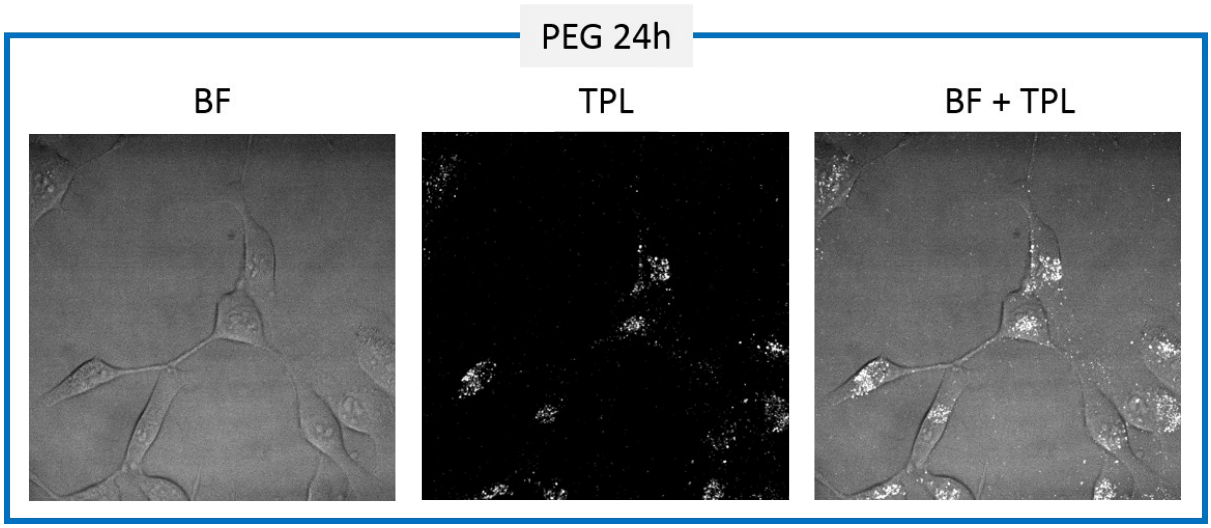

Figure S3. Bright-field (BF), two-photon luminescence (TPL) and superimposition (BF+TPL) images from *in vitro* uptake of GNR-PEG 24 hours after incubation with 786-O cells.

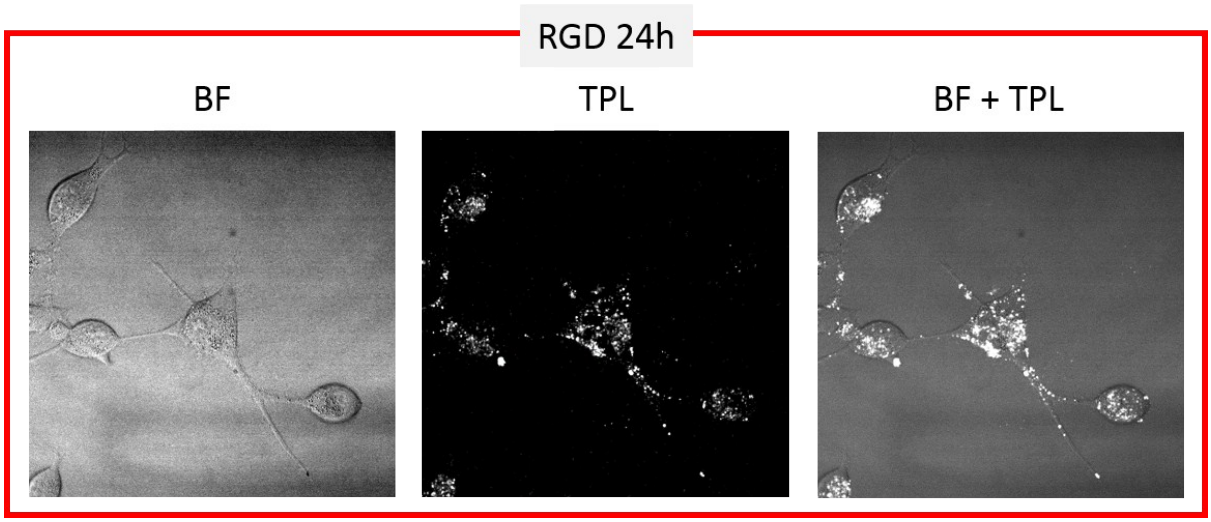

Figure S4. Bright field (BF), two-photon luminescence (TPL) and superimposition (BF+TPL) images from *in vitro* uptake of GNR-RGD 24 hours after incubation with 786-O cells.

IN VIVO MODEL AND GOLD NANOROD INJECTION

An orthotopic renal cell carcinoma tumor was originally generated in immunosuppressed mice (male athymic nude mice, Harlan Laboratories). 5-6-week-old mice were anesthetized, left kidney exteriorized and $1x10^6$ cells 786-O cell line (human clear cell renal cell adenocarcinoma, ATCC CRL-1932) were directly injected into kidney capsule (original neoplastic organ). Once tumor was palpable, (approximately 1,000 mm^3 of volume) animals were sacrificed and a 3-5 mm^3 of volume piece of tumor was laid on the top of exteriorized kidney of new recipient and stitched in using surgical sutures. When tumor reached 1000 mm^3, 100 µL of physiological serum 0.9% (B.Braun, Rubí, Spain), GNR-PEG or GNR-RGD were injected. GNRs were diluted with physiologic serum at 21 nM before injection. In each dose, 110 µg of gold (4 mg/Kg, 1 mg/mL or 10^{12} GNRs) were injected considering GNRs of

$52 \cdot 10^6$ Dalton (gr/mol) of molecular weight. This concentration of GNRs is not toxic at least up to six months after injection (data not shown).

All animal experiments have been developed at Catalan Institute of Oncology (ICO) in IDIBELL AAALAC-accredited facility, according to our Institute's Animal Research Committee acceptance (CEEA #4899) and approved by Catalan Government ethics committee (CEA project # 9727).

INDUCTIVELY COUPLED PLASMA MASS SPECTROSCOPY

The gold concentration in tissue from half of each organ not used for TPL microscopy were analyzed with an inductively coupled plasma mass spectrometer (ICP-MS) system (Optima 8300, Perkin Elmer) in the Unitat d'Anàlisi de Metalls Centres Científics i Tecnològics at Universitat de Barcelona (CCiTUB).

Tissue (maximum 300 mg of each sample) was digested in a reactor in HNO_3, H_2O_2 and HCl at 90^{o}C and then, diluted with HCl and thiourea. Five certified gold concentrations from the national institute of standards and technology (NIST) and three blanks were used as a calibration of the systems. The units in the results are grams of gold per grams of sample. The estimated error of the mean gold concentration per gram of tissue was 5%.

TWO-PHOTON LUMINESCENCE OF ANIMAL TISSUES

We demonstrated the potential of calibrated TPL imaging to quantify the concentration of GNR with different contrast injection (GNR-PEG and GNR-RGD) in different organs compared to the ICP-MS quantification (Figure S5). Control group (CTL) images from one mouse injected with saline solution (PBS) was shown in Figure S6. Distribution of GNR-PEG and GRN-RGD in tumor 6 hours and 24 hours after tail injection was shown in Figure S7. TPL images of tail injected GNR-RGD after 24 hours in kidney, tumor, spleen and liver are shown in Figure S8.

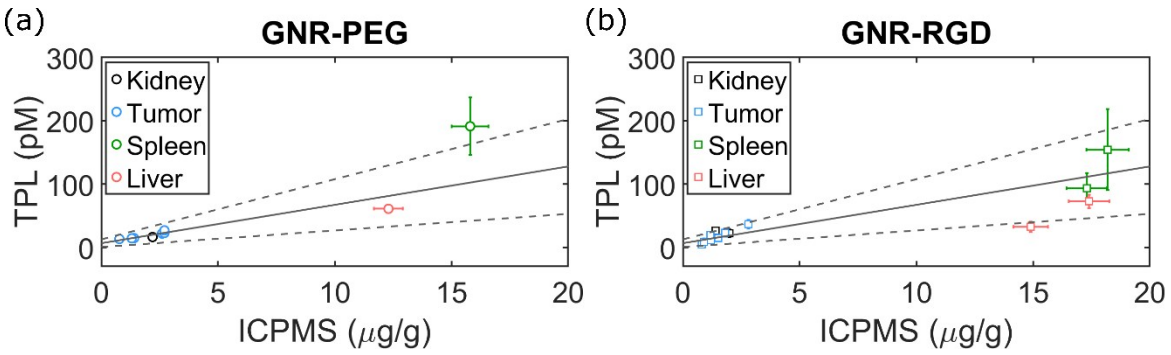

Figure S5. Deming linear slope between concentration of gold and GNRs (GNR-PEG in (a), GNR-RGD in (b)) in biopsied tissues (kidney, tumor, spleen and liver) analyzed with inductively coupled mass spectroscopy (ICP-MS, in μg/g) and TPL microscopy (in pM), respectively. In grey, Deming linear fitting (R2 = 0.69 and p-value << 0.001) and 95% confidence interval are represented. Mice 24 hours after tail vein injection of 100 μL GNR-PEG or GNR-RGD (both at 21 nM). Mean and standard deviation are shown.

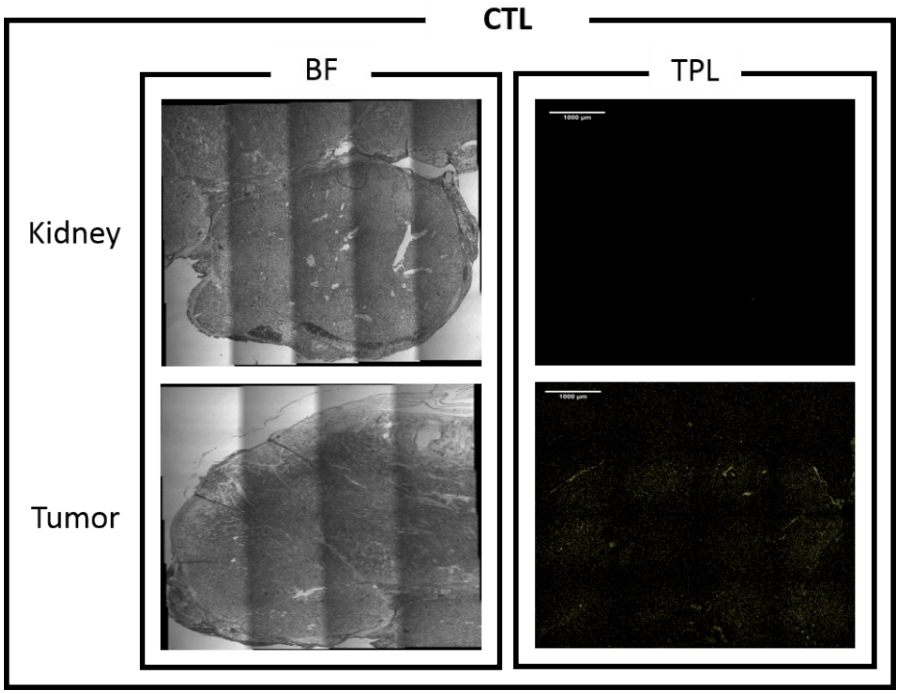

Figure S6. Bright field (BF) and two-photon luminescence (TPL) images of paraffined tissue from the kidney and the tumor of mice injected with saline solution. Scale bar is 1 mm.

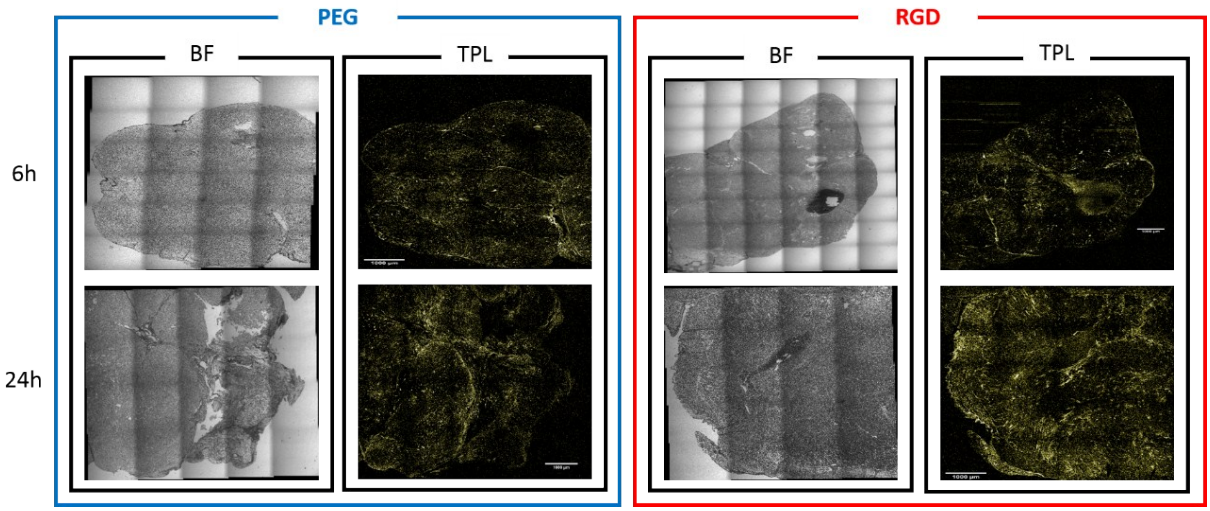

Figure S7. Bright field (BF) and two-photon luminescence (TPL) images of paraffined tissue from the tumor of mice 6 hours and 24 hours after injection of 100 µL GNR-PEG and GNR-RGD at 21 nM. From the images, subtle differences in distribution and quantification of GNRs was shown. Scale bar is 1 mm.

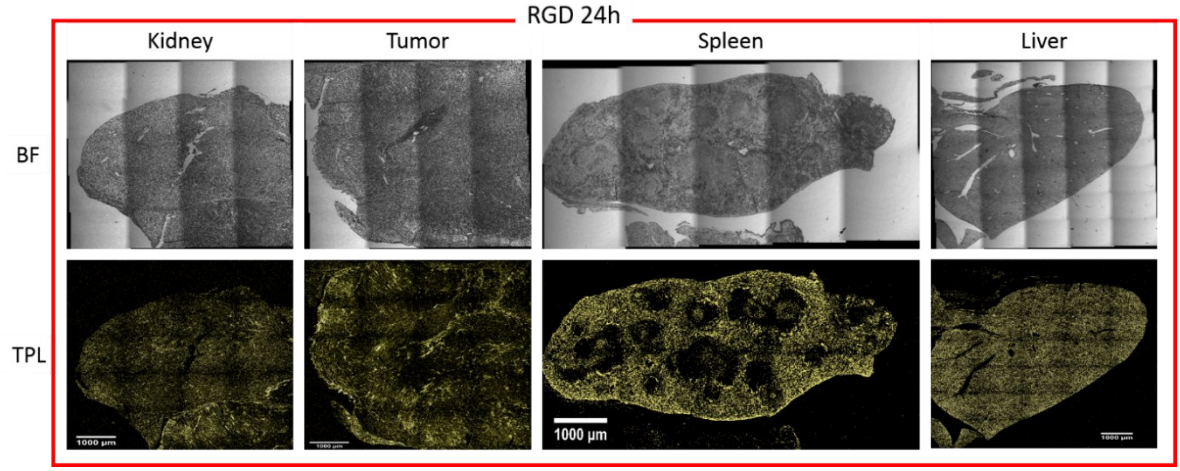

Figure S8. Bright field (BF) and two-photon luminescence (TPL) images of paraffined tissues from Kidney, tumor, spleen and liver of a mouse sacrificed 24 hours after injection of 100 µL of GNR-RGD at 21 nM. Different organs showed peculiar sub-organ distributions and accumulations of GNRs. Scale bar is 1 mm.

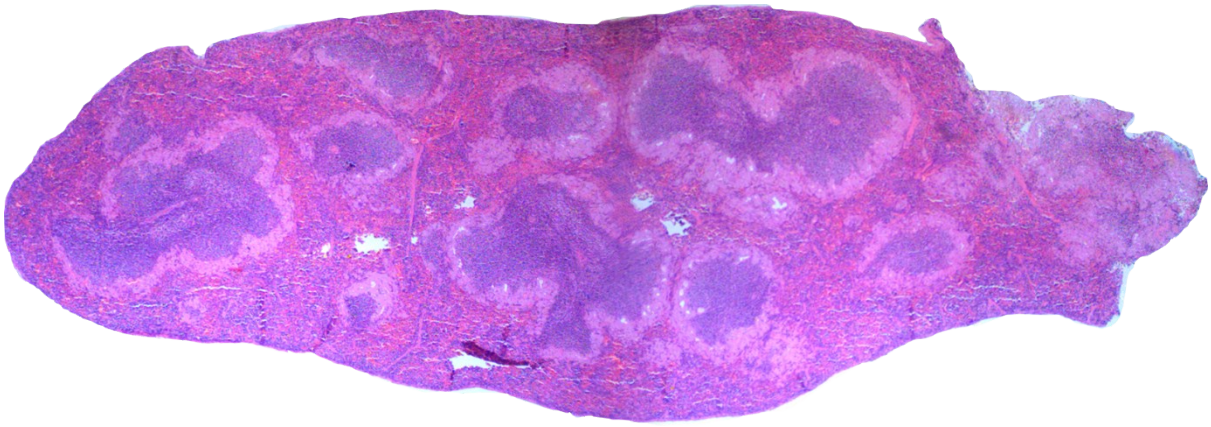

Figure S9. Hematoxylin and eosin staining of spleen of a mouse sacrificed 24 hours after injection of 100 µL of GNR-RGD at 21 nM. Red and white pulp areas are distinguishable.

BIBLIOGRAPHY

(1) Wilhelm, S.; Tavares, A. J.; Dai, Q.; Ohta, S.; Audet, J.; Dvorak, H. F.; Chan, W. C. W. Analysis of Nanoparticle Delivery to Tumours. *Nat. Rev. Mater.* **2016**, *1*, 1–138.

(2) Liu, X.; Huang, N.; Li, H.; Wang, H.; Jin, Q.; Ji, J. Multidentate Polyethylene Glycol Modified Gold Nanorods for in Vivo Near-Infrared Photothermal Cancer Therapy. *ACS Appl. Mater. Interfaces* **2014**, *6*, 5657–5668.

(3) Niidome, T.; Yamagata, M.; Okamoto, Y.; Akiyama, Y.; Takahashi, H.; Kawano, T.; Katayama, Y.; Niidome, Y. PEG-Modified Gold Nanorods with a Stealth Character for in Vivo Applications. *J. Control. Release* **2006**, *114*, 343–347.

(4) Niidome, T.; Akiyama, Y.; Yamagata, M.; Kawano, T.; Mori, T.; Niidome, Y.; Katayama, Y. Poly(Ethylene Glycol)-Modified Gold Nanorods as a Photothermal Nanodevice for Hyperthermia. *Journal of Biomaterials Science, Polymer Edition*, 2009, *20*, 1203–1215.

(5) Lipka, J.; Semmler-Behnke, M.; Sperling, R. A.; Wenk, A.; Takenaka, S.; Schleh, C.; Kissel, T.; Parak, W. J.; Kreyling, W. G. Biodistribution of PEG-Modified Gold Nanoparticles Following Intratracheal Instillation and Intravenous Injection. *Biomaterials* **2010**, *31*, 6574–6581.

(6) Huang, X.; Peng, X.; Wang, Y.; Wang, Y.; Shin, D. M.; El-Sayed, M. A.; Nie, S. A Reexamination of Active and Passive Tumor Targeting by Using Rod-Shaped Gold Nanocrystals and Covalently Conjugated Peptide Ligands. *ACS Nano* **2010**, *4*, 5887–5896.

(7) de Melo-Diogo, D.; Pais-Silva, C.; Dias, D. R.; Moreira, A. F.; Correia, I. J. Strategies to Improve Cancer Photothermal Therapy Mediated by Nanomaterials. *Adv. Healthc. Mater.* **2017**, *6*.

(8) Yu, M.; Zheng, J. Clearance Pathways and Tumor Targeting of Imaging Nanoparticles. *ACS Nano*, 2015, *9*, 6655–6674.